25th ABCM International Congress of Mechanical Engineering
October 20-25, 2019, Uberlândia, MG, Brazil

NUMERICAL FLOW SIMULATION IN NATURALLY FRACTURED PETROLEUM RESERVOIRS USING A MPFA-STREAMLINE FORMULATION

Kelly Cristinne Leite Angelim
Túlio de Moura Cavalcante
Jonathan da Cunha Teixeira
Paulo Roberto Maciel Lyra
Darlan Karlo Elisiário de Carvalho

Federal University of Pernambuco. Av. Acadêmico Hélio Ramos s/n, CEP: 50670-901, Recife, PE, Brazil
kellyangelim01@gmail.com
tulio.cavalcante5@yahoo.com
jonathan.lmcg@gmail.com
prmlyra@padmec.org
dkarlo@uol.com.br

Abstract. *Numerical simulation of fluid flows in petroleum reservoirs is a fundamental tool with great applicability in the oil industry. Naturally fractured reservoirs have great structural and geometric complexity that makes it difficult to use structured meshes to adequately represent these systems, requiring the use of unstructured meshes. In this paper, we present a numerical formulation to simulate two-phase flow of oil and water in naturally fractured oil reservoirs using unstructured quadrilateral meshes. For the resolution of the diffusive pressure problem, we have used a Finite-Volume Method with a Multipoint Flux Approximation with a Diamond stencil (MPFA-D), which represents a very robust and flexible formulation that is capable to deal with highly heterogeneous fractured domains and full permeability tensor representation of the rock matrix in any polygonal grid. For the approximation of the advective saturation problem, we used the streamline-based method, which is very efficient due to the decoupling of the transport equations from 2-D into multiple 1-D problems that are solved along each streamline, reducing drastically the computational cost. These methods were implemented in the context of the Hybrid Dimensional (HyD) Grid Model. In order to validate the proposed formulation, we solve some benchmark problems found in literature.*

Keywords: *Naturally Fractured Reservoirs; Two-Phase Flows of Oil and Water; MPFA-D; Streamline Method.*

1. INTRODUCTION

Numerical simulation is a strategic tool for planning and managing the production of oil reservoirs, predicting its behavior in relation to the pressure, temperature and flow of fluids in the porous medium (Aziz and Settari, 1979). The modelling of oil and water displacements in porous media can be described by an elliptic pressure equation and by a hyperbolic saturation equation that are coupled by the total velocity field (Peaceman, 1977). This approach allows the use of numerical methods that are more efficient and accurate in the context of multiphase flow simulation in oil reservoirs (Kozdon et al., 2011).

In the present paper, to solve the elliptic pressure equation, we use the Multipoint Flux Approximation Method with a Diamond Stencil (MPFA-D). This method was presented by Gao and Wu (2010) and further adapted for the simulation of two-phase flows in petroleum reservoirs by Contreras et al. (2016). This method presents a robust and flexible formulation capable of dealing with highly heterogeneous and anisotropic domains, as in the cases of naturally fractured reservoirs, adapted for general polygonal meshes.

Reservoirs whose fractures significantly interfere in the flow pattern are called naturally fractured reservoirs (Firoozabadi, 2000). In these systems, it is particularly complex to use structured meshes which are capable to properly model the reservoir, requiring methods capable to deal with unstructured meshes and anisotropic (full tensor) permeability. In the Hybrid-Dimensional Grid Model (HyD), the mesh generation needs to fit the fractures positions, so that the fractures are mesh edges. In these methods, the fractures are expanded to *n*-dimensional on the computational domain and the equations for the fractures and the matrix are discretized together (Cavalcante et al., 2018).

In addition, to deal with complex geologic models that demand a high computational cost, to solve the transport equation, streamline-based simulations have received increased attention in the last years (Haegland et al., 2007; Chen

et al., 2018). In the streamline method, the pressure distribution is obtained implicitly over the Eulerian grid and then the streamlines are drawn using Pollock's semi-analytical method. Afterwards, the transport equations are solved explicitly along the streamlines over the Lagrangian domain (time-of-flight grid). Because the equations are one-dimensional along the streamlines, the number of calculations and, therefore, the amount of memory required for simulation is smaller than in conventional methods (Mesbah et al., 2018).

In this context, in the present paper, we propose a numerical formulation to simulate two-phase flows of oil and water in naturally fractured oil reservoirs, using an adaptation of the MPFA-D to the Hybrid Dimensional Grid Model to implicitly solve the elliptic pressure equation and applying a streamline-based method in the resolution of the hyperbolic transport equation, using unstructured quadrilateral meshes.

2. MATEMATICAL FORMULATION

In this section, the equations that are used to model the two-phase flow (oil and water) in heterogeneous and anisotropic petroleum reservoirs are briefly presented. The model considers isothermal, incompressible fluid flow and porous media, and that the effects of gravity and capillarity can be neglected.

The mass balance equation (Bear, 1972) can be given by:

$$\phi\rho_i \frac{\partial S_i}{\partial t} + \rho_i \vec{\nabla}\cdot\vec{v}_i = q_i \tag{1}$$

and using the Darcy's Law (Peaceman, 1977; Ewing, 1983):

$$\vec{v}_i = -\lambda_i \underset{\sim}{K} \vec{\nabla} p_i \tag{2}$$

where i is the phase index, for water (w) or oil (o), ϕ is the porosity, t is the time variable, $\vec{\nabla}$ is the gradient operator, ρ_i, S_i, $\vec{v}_i$, q_i are, respectively, the phase density, phase saturation, velocity and source term of each phase i, λ_i is its mobility, given by the ratio $\lambda_i = k_{ri}/\mu_i$, where k_{ri} is its relative permeability and μ_i is its viscosity. $\underset{\sim}{K}$ is the absolute permeability tensor and p_i is the pressure. Brooks and Corey type relative permeabilities (Kozdon et al., 2011) are used, and defined by:

$$k_{rw} = \left(S_e\right)^{n_w}; \quad k_{ro} = \left(1 - S_e\right)^{n_o} \tag{3}$$

where n_w and n_o are exponents that can assume different values, S_e is the effective saturation which is a normalization of the wetting phase saturation with respect to the irreducible water saturation (S_{wi}) and the residual oil saturation (S_{or}). It is defined by (Chen et al., 2006):

$$S_e = \frac{S_w - S_{wi}}{1 - S_{wi} - S_{or}} \tag{4}$$

Considering that the media only contains oil and water, it is possible to write the following restrictive equation:

$$S_w + S_o = 1 \tag{5}$$

Writing Eq. (1) for both phases and applying the restriction from the Eq. (5) to eliminate the saturation, and after some algebraic manipulation, the elliptic pressure equation (Peaceman, 1977; Contreras et al., 2016) is given as:

$$\vec{\nabla}\cdot\vec{v} = Q \quad (\text{with } \vec{v} = -\lambda \underset{\sim}{K} \vec{\nabla} p) \tag{6}$$

where $\vec{v} = \vec{v}_w + \vec{v}_o$, is the total velocity and the specific total flow rate is $Q = Q_w + Q_o$, where $Q_i = q_i/\rho_i$, with $i=w,o$. Moreover, $\lambda = \lambda_w + \lambda_o$ is the total mobility and p is the global pressure, neglecting capillarity effects. The fractional flow of a phase is defined as $f_i = \lambda_i/\lambda$, so the velocity of a phase is $\vec{v}_i = f_i\vec{v}$. Therefore, the Eq. (1) for the water phase can be written (Peaceman, 1977; Chen et al., 2006) as:

$$\phi \frac{\partial S_w}{\partial t} + \vec{\nabla} \cdot \left(f_w \vec{v} \right) = Q_w \tag{7}$$

This Eq. (7) is the hyperbolic saturation equation. Equations (6) and (7) are coupled by the total velocity field $\vec{v}$.

2.1 Initial and Boundary Conditions

In order to get a complete description of the problem, it is necessary to define appropriate initial and boundary conditions. In this case, considering a domain Ω, its contour Γ is defined as:

$$\Gamma = \Gamma_D \cup \Gamma_N \cup \Gamma_P \cup \Gamma_I \tag{8}$$

where Γ_D and Γ_N represent the boundaries with prescribed pressures (Dirichlet boundary conditions), and prescribed fluxes (Neumann boundary conditions), respectively, Γ_P and Γ_I are the production and injection wells, respectively. Therefore, these conditions are typically given by (Aziz and Settare, 1979; Contreras et al., 2016):

$$\begin{aligned} &p\left(\vec{x},t\right) = g_D && \text{on } \Gamma_D \times [0,t] \\ &\vec{v} \cdot \vec{n} = g_N && \text{on } \Gamma_N \times [0,t] \\ &S_w\left(\vec{x},t\right) = \overline{S}_w && \text{on } \Gamma_I \times [0,t] \\ &S_w\left(\vec{x},0\right) = \overline{S}_w^0 && \text{on } \Omega \end{aligned} \tag{9}$$

where $\vec{x}$ represents the position vector, t is the time variable, g_D is a scalar functions for pressure and g_N is a scalar function for flux. Moreover, $\vec{n}$ is the outward unitary normal vector to the control surface, $\vec{v}$ is the total velocity and $\overline{S}_w$ is the prescribed saturation on an injection well.

3. NUMERICAL FORMULATION

In what follows, the numerical strategies used to discretize the pressure and saturation equations and the solution procedure proposed are briefly presented, which is a variant of the IMPES approach, called MIMPES (Modified IMplicit Pressure Explicit Saturation) (Hurtado et al., 2006; Da Silva et al., 2016).

3.1 Pressure Equation

The discretization of the pressure equation is performed by the MPFA-D. Integrating Eq. (6) into a control volume (CV) and using the Gauss divergence theorem, we have:

$$\int_{\Omega} \vec{\nabla} \cdot \vec{v} \; dV = \int_{\partial\Omega} \vec{v} \cdot \vec{n} \; dA = \sum_{i}^{Z_i} \vec{v}_i \cdot \vec{N}_i = \overline{Q} V \tag{10}$$

where $\vec{n}$ is the outward unitary normal vector to the control surface, V is the cell volume (or area, in 2-D), A is the area (or length, in 2-D) of the cell faces and $\overline{Q}$ is the mean source term, Z_i indicates the amount of edges of the i-th cell.

To obtain the flux expression for one control surface (edge in 2-D) of the mesh, we construct the MPFA-D stencil, as depicted in Figure 1.

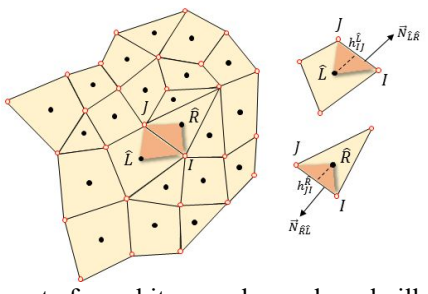

Figure 1. Local diagram of a part of an arbitrary polygonal mesh, illustrating the "diamond stencil".

After some algebraic manipulation, the flux continuity equation can be written as (Gao and Wu, 2010; Contreras et al., 2016):

$$\vec{v}_{IJ} \cdot \vec{N}_{IJ} = \tau_{IJ} \left[p_{\hat{R}} - p_{\hat{L}} - \upsilon_{IJ} \left(p_J - p_I \right) \right] \tag{11}$$

where

$$\tau_{IJ} = -\lambda_{IJ} \frac{K_{IJ_{\hat{L}}}^{(n)} K_{IJ_{\hat{R}}}^{(n)}}{K_{IJ_{\hat{L}}}^{(n)} h_{JI}^{\hat{R}} + K_{IJ_{\hat{R}}}^{(n)} h_{IJ}^{\hat{L}}} \left| \overrightarrow{IJ} \right|; \quad \upsilon_{IJ} = \frac{\overrightarrow{\hat{L}\hat{R}} \cdot \overrightarrow{IJ}}{\left| \overrightarrow{IJ} \right|^2} - \frac{1}{\left| \overrightarrow{IJ} \right|} \left(\frac{K_{IJ_{\hat{L}}}^{(t)}}{K_{IJ_{\hat{L}}}^{(n)}} h_{IJ}^{\hat{L}} + \frac{K_{IJ_{\hat{R}}}^{(t)}}{K_{IJ_{\hat{R}}}^{(n)}} h_{JI}^{\hat{R}} \right) \tag{12}$$

In Eq. (11), $p_{\hat{R}}$ and $p_{\hat{L}}$ are approximations of pressure in the barycenters of the righ and left control volumes (CVs) of edge *IJ*. Moreover, the nodal pressures, p_I and p_J are computed using the pressure values of the CVs surrounding nodes *I* and *J*, respectively, via a Linear Preserving Weighted Interpolation (Contreras et al., 2016)

3.2 Saturation Equation

When using a streamline-based simulation, Eq. (2) is rewritten in terms of time-of-flight (TOF) τ , which represents a coordinate along the streamline, intuitively turning a 2D/3D transport problem as a sum of 1D decoupled simulations solved along the streamlines (Datta-Gupta and King, 2007).

The τ is the time taken by a neutral particle tracer to traverse a specific distance s along a streamline traced ξ based on the velocity field $\vec{v}(\xi)$ and is given by Eq. (13):

$$\tau = \int_0^s \frac{\phi(\xi)}{\left| \vec{v}(\xi) \right|} d\xi \tag{13}$$

Blunt et al. (1996) outlined the following coordinate transform by first differentiate the two sides for s in Eq. (13) as:

$$\frac{\partial \tau}{\partial s} = \frac{\phi}{\left| \vec{v} \right|} \tag{14}$$

which can further be rewritten as:

$$\vec{v} \cdot \nabla = \phi \frac{\partial}{\partial \tau} \tag{15}$$

Applying Eq. (15) in Eq. (7) and after some algebraic manipulation we are be able to apply the streamline-based method allowing rewriting the saturation equation as (Batycky, 1997; Datta-Gupta and King, 2007; Chen et al., 2018):

$$\frac{\partial S_w}{\partial t} + \frac{\partial f_w}{\partial \tau} = 0 \tag{16}$$

More details regarding the coordinate transformation and the streamline construction can be found in Thiele et al. (1996), Batycky (1997) and Datta-Gupta and King (2007).

In the streamline method, we need to trace the streamlines based on a divergence-free velocity field obtained from the MFPA-D method. In this work, we follow the approach presented by Jimenez et al. (2007), where we use a reconstruction of the total MFPA-D fluxes and the Piola transformation (Cordes and Kinzelbach,1992) with fluxes mapped from the physical to the reference space, as illustrated in Figure 2, by evaluating the velocities (at the reference space) as linear combinations of continuous fluxes across cell faces in the normal direction. Then, we trace the streamline path analytically using the standard Pollock (1988) method.

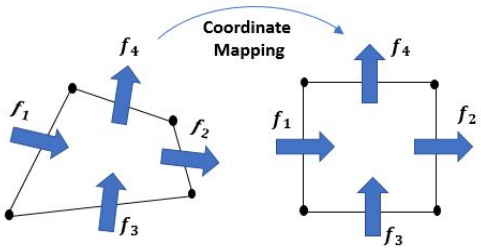

Figure 2. Location of fluxes on the reference control volume.

In the calculation of streamline trajectories and time of flight (TOF) by Pollock (1988) method, each grid block is a rectangular cell, and the transit time from an initial point in space is built up one cell at a time and a single uniform velocity approximation is applied to each face. This approach is generalized for unstructured grids by Cordes and Kinzelbach (1992), and further simplified by Jimenez et al. (2007) by introducing a parameter *T*, called the *pseudo time of flight*, which is simply the time of flight normalized by the Jacobian of the transformation,

$$dT = \frac{1}{\phi}\frac{d\tau}{\mathrm{J}(\alpha,\beta)} = \frac{d\alpha}{Q_1(\alpha)} = \frac{d\beta}{Q_2(\beta)} \tag{17}$$

where τ is the time of flight, (α,β) are unit space coordinates, J is the Jacobian matrix of the isoparametric mapping from physical space (x,y) to the unitary space (α,β), and $Q_1(\alpha)$ $Q_2(\beta)$ are the fluxes along two directions.

These sets of equations can be independently integrated along each direction. The integral solution of the exit pseudo time in the α direction is given, by:

$$\Delta T_\alpha = \int_{\alpha_o}^{\alpha=1}\frac{d\alpha}{Q_1(\alpha)} = \int_{\alpha_o}^{\alpha=1}\frac{d\alpha}{a_1+c_1\alpha} = \frac{1}{c_1}\ln\left[\frac{a_1+c_1\alpha}{a_1+c_1\alpha_0}\right]\Bigg|_{\alpha=1} = \frac{1}{c_1}\ln\left[\frac{a_1+c_1}{a_1+c_1\alpha_0}\right] \tag{18}$$

Similar solution will also apply in β direction. The final pseudo time of flight at the exit point of cell is given by minimum positive value among the exit pseudo times in all directions,

$$\Delta T = \min\left\{\Delta T_\alpha, \Delta T_\beta\right\} \tag{19}$$

After the exit time is determined inside the cell, the exit point coordinates can be easily calculated. The α coordinate of the exit point is

$$\alpha_e = \alpha_0 + (a_1 + c_1\alpha_0)\left(\frac{e^{c_1\Delta T}-1}{c_1}\right) \tag{20}$$

Similar solution also applies along the β direction. Once we know the unitary space coordinates of the exit point, the corresponding physical space coordinates can be obtained via bilinear interpolation (Datta-Gupta and King 2007). The equations of the streamlines path in the physical cell is obtained by carrying out the integrals in Equation (17) in analogously to the Pollock's method. For more details regarding the derivation, see Jimenez et al. (2007) and Datta-Gupta and King (2007). After obtaining the trajectory, the τ on physical space is determined using

$$\tau = \phi\int_0^T J[\alpha(T),\beta(T)]dT \tag{21}$$

The trajectory and time-of-flight formulation recognizes the importance of taking into account the variation in the Jacobian within the cell to accurately reflect the velocity variations along a trajectory, hence, a rigorous tracing is performed within highly non-orthogonal cells (Jimenez et al. 2007). A complete streamline trajectory is obtained by repeating this single cell tracing procedure cell by cell until a termination point is found, such as a well cell, a stagnation point, and so on (Chen et al., 2018).

For each streamline traced, we record the time necessary to cross the current CV. Thus, the full-dimensional transport equation (2-D or 3-D) is transformed into a set of one-dimensional equations along the streamlines in terms of

time-of-flight, Eq. (6), which is discretized along the streamlines, using a simple first order upstream (FOUM) weighting as in Eq. (22):

$$S_w^{i,n+1} = S_w^{i,n} + \frac{\Delta t_{sl}}{\Delta \tau}\left[f_w^{i,n} - f_w^{i-1,n} \right] \tag{22}$$

where i is a cell identifier along the discretized streamline and n is the time level and Δt_{sl} is the time step used in the streamline solution, satisfying the CFL criterion (Hirsch, 1994), and it is given by:

$$\Delta t_{sl} = \frac{n_{CFL}\Delta \tau}{v_{\max}^{w}} \tag{23}$$

in which $n_{CFL} \leq 1$ is the Courant number and $v_{\max}^{w}$ represents the maximum shock velocity defined as (Datta-Gupta and King, 2007):

$$v_{\max}^{w} = \left[\frac{(f_w^{sl})_i^n - (f_w^{sl})_{i-1}^n}{(s_w^{sl})_i^n - (s_w^{sl})_{i-1}^n} \right] \tag{24}$$

Once all streamlines are traced, the values of the saturation are obtained along them. They are mapped from the streamline grid to the underlying simulation grid to approximate the physical properties back on the individual CV. For this purpose, we employ a weighted averaging approach (Batycky, 1997; Datta-Gupta and King, 2007), i.e., the phase saturation associated to a control volume is calculated using the weighted average of the saturation of the streamlines passing through that CV, which is calculated as:

$$S_w^{CV} = \frac{\sum_{i=1}^{n_{CV}^{sl}} [\Delta \tau_i \cdot \overline{S}_w^{i,sl}]}{\sum_{i=1}^{n_{CV}^{sl}} \Delta \tau} \tag{25}$$

where S_w^{CV} is the saturation of control volume CV, n_{CV}^{sl} number of streamlines passing through the CV under consideration, $\Delta \tau_i$ is time necessary to cross that CV, $\overline{S}_w^{i,sl}$ is the average saturation for the i^{th} streamline.

3.3 Hybrid-Dimension Grid Fracture Model

The hybrid-dimensional grid model consists on the explicit representation of the fractures, in the geometric mesh, as lower-dimensional entities and expand them to the same dimension of the mesh in computational domain, so equations for the fractures and for the rock matrix can be discretized together (Sandve et al., 2012; Ahmed et al., 2017; Cavalcante et al., 2018). The construction of the hybrid-dimensional grid, i.e., the computational grid in which the fractures are dimensionally expanded, for this work, which uses just 2-D meshes, was made by the scheme shown in Fig. (3) and following the procedure explained below (Cavalcante et al., 2018).

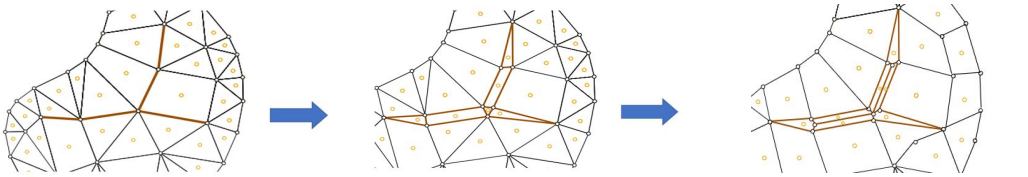

(a) Original grid (b) Mixed hybrid-grid (b) Quadrilateral hybrid-grid

Figure 3. Hybrid-grid construction.

Considering the original grid (Fig 3a), in the vicinity of each fracture-edge (geometric mesh edge representing a fracture), two parallel straight auxiliary lines must be traced, each one at the distance of half of the aperture set for that fracture (Fig. 3b). Each internal point that is shared by at least two fracture-edges becomes z new points, where z is the amount of edges sharing the evaluated node. Then, each new point will be determined by the intersection of the segments parallel to the fracture edges. For example, if a node is shared by three fracture-edges, it becomes a triangle

element (Fig. 3b). In the case of quadrilateral meshes, to eliminate the triangular elements formed by a node that shares three fracture edges, it is necessary to use an additional node. Consequently, the internal elements in the fracture will divide resulting in a local refinement, which is, relatively, computationally inexpensive. Therefore, the internal nodes will become new points defined by the intersection of the parallel segments with the edge of the fracture (Fig. 3c). After the computational hybrid-grid is defined, we can just proceed solving the *n*D pressure equations by using the MPFA-D method.

4. RESULTS

In this section, we present some results of the application of our MPFA-streamline formulation using a hybrid representation of the grid (MPFA-SF-HyG) to simulate some representative two-phase flow problems in 2-D naturally fractured reservoirs. In all problems, the model consists of the classical 2-D ¼ of five-spot configuration. The domain is defined as $\Omega = [0,1] \times [0,1]$ m and different arrangement of matrix and fractures are considered for each example. The injection well placed in the bottom-left corner of the domain with a constant unit flow rate the producer well is located at the top-right corner of the domain with a constant zero pressure. No-flow boundary conditions are applied in all four external boundaries of the reservoir. In all examples, water and oil viscosities are, respectively, $\mu_w = 1$ and $\mu_o = 1$. Water and oil densities are, respectively, $\rho_w = 1$ and $\rho_o = 1$. Moreover, the exponents n_w and n_o of Eq. 3 are always equal to 2, the porosities are always set as 0.5 in the rock matrix and 1 in the fractures e the Courant number is 0.8. The rock matrix properties are referred to by the subscript *m* and the fracture properties are referred to by the subscript *f*.

4.1 The ¼ five spot two-phase flow with single diagonal fracture

In this example we have a single diagonal fracture with aperture $a_f = 10^{-4}$ and the rock matrix permeability is K_m which are given by:

$$K_m = \begin{bmatrix} 1 & 0 \\ 0 & 1 \end{bmatrix} \tag{26}$$

The permeability in the fracture K_f is:

$$K_f = 10^{-16} K_m \tag{27}$$

In Figure 4a we present the unstructured grid with 1597 control volumes and in Fig. 4b the streamline tracing in the fractured domain. We can note that the streamlines surround the region of low permeability (fracture), as expected, avoiding any barrier inside the domain.

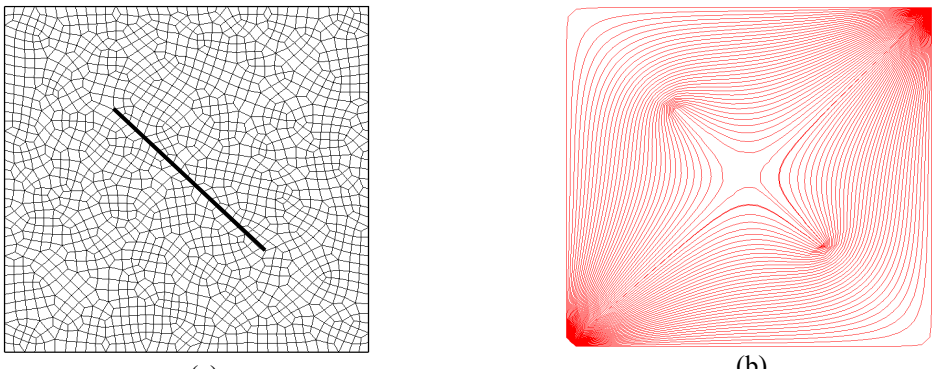

(a) (b)

Figure 4. Mesh used in this test case (a) and streamline tracing in a fractured domain (b).

In order to evaluate of the robustness of our formulation, we have compared our results with the results obtained using the MPFA-D/HyG coupled to the traditional First Order Upwind Method (FOUM), presented by Cavalcante et al. (2018). In Figure 5, we present the pressure and the saturation fields for 0.3 PVI (Pore Volume Injected). As it can be seen in Figs. 5b and 5d, results are quite similar for both strategies. Comparing the the results for the two formulations the pressure and the saturation profiles are very close to each other, but it is possible to identify some qualitative differences. Clearly the MPFA-D/SF-HyG produces a saturation profile that is less diffusive than the MPFA-D/FOUM-

HyG with a very small anticipation of the water breakthrough for the MPFA-D/SF-HyG as it can be seen in Fig. 6b. Therefore, this example provides an important evidence of the robustness of our formulation, which shows to be capable to deal with a problem with a fractured domain on a fully unstructured grid.

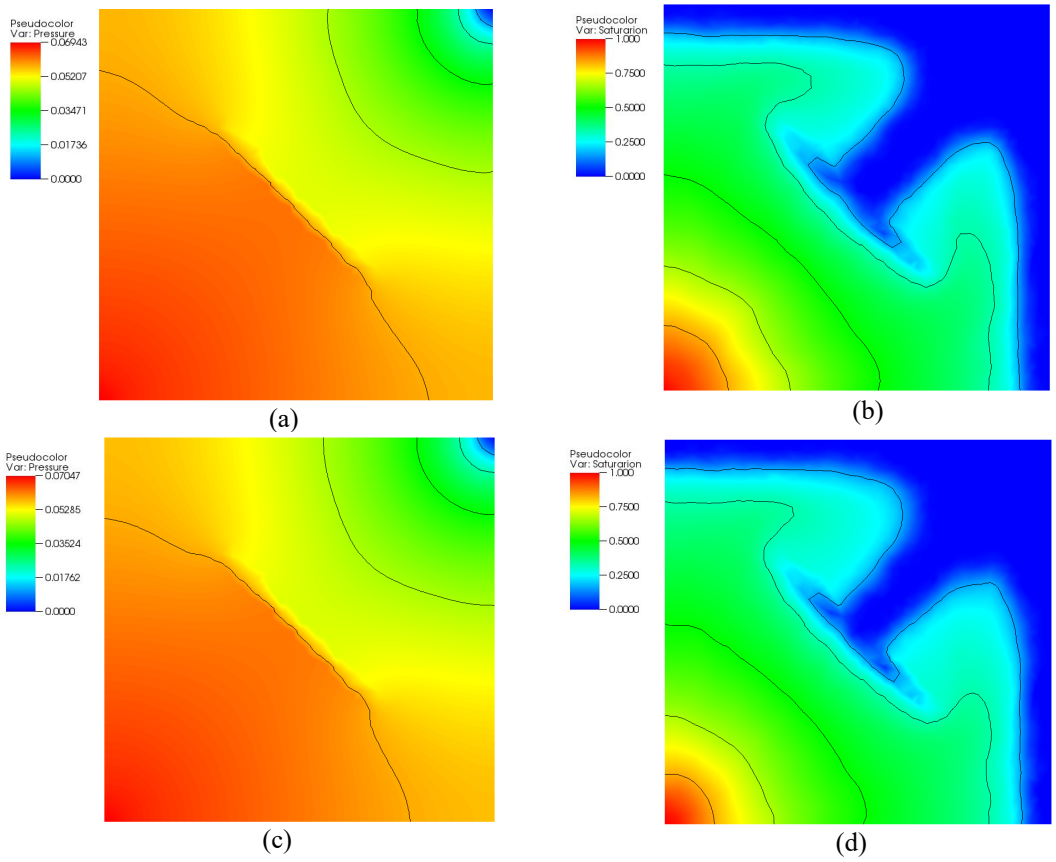

Figure 5. Pressure and Saturation fields for the for the ¼ of five-spot problem with a diagonal fracture at t = 0.3 PVI: (a) Pressure field using the MPFA-D/SF-HyG; b) Saturation field using the MPFA-D/SF-HyG; (c) Pressure field using the MPFA-D/FOUM-HyG; d) Saturation field using the MPFA-D/FOUM-HyG.

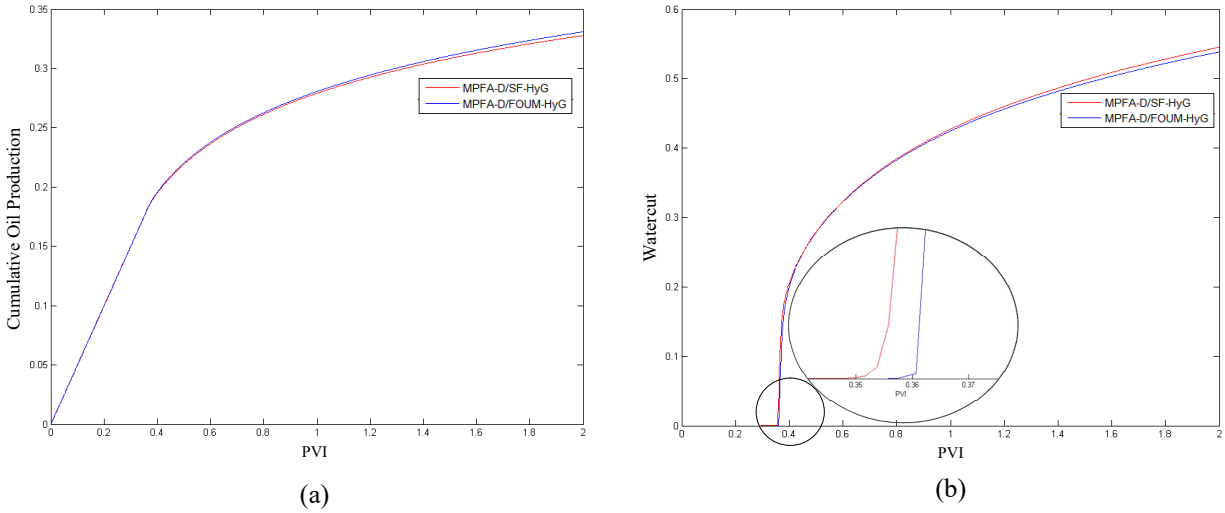

Figure 6. Production report for the ¼ five spot two-phase flow problem with a diagonal fracture. (a) Cumulative Oil Production. (b) Watercut and zoom in the breakthrough region

4.2 The ¼ five spot two-phase flow with connected channel and barriers

In this example, we test our formulation (MPFA-D/SF-HyG) for a ¼ of five-spot problem adapted from Cavalcante et al. (2018). The domain is represented with the diagonal channel (high permeability fracture) connected with barriers (low permeabilities fractures) and discretized by 566 quadrilaterals cells (See Fig. 7). The rock matrix permeability

K_m is the same as given in the previous example and the permeability in the channel is $K_{f_1} = 8 \cdot 10^7 K_m$ and the permeability in the barriers is $K_{f_2} = 10^{-16} K_m$. The aperture of the fractures (channels and barriers) is $a_f = 10^{-3}$.

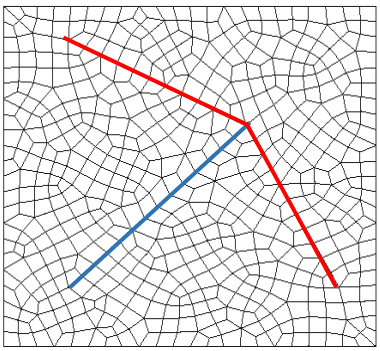

Figure 7. Mesh used in this test case highlighting for channel (blue line) and barrier (red lines)

Figure 8a shows an accentuated pressure gradient, evidencing how the presence of fractures modifies the pressure field of the domain. Moreover, it is possible to note in Fig 8b that the streamlines enter the channel (high permeability zone) and surround the barrier (low permeability zone). Note that the water saturation front need to walk around the barriers (Fig. 8c) and, because of this, the water can sweep more oil from the reservoir, increasing the cumulative oil production (Fig. 9a) and retarding of the water breakthrough (Fig. 9b). Again, we see that our results match quite well with those obtained using the MPFA-D/FOUM-HyG.

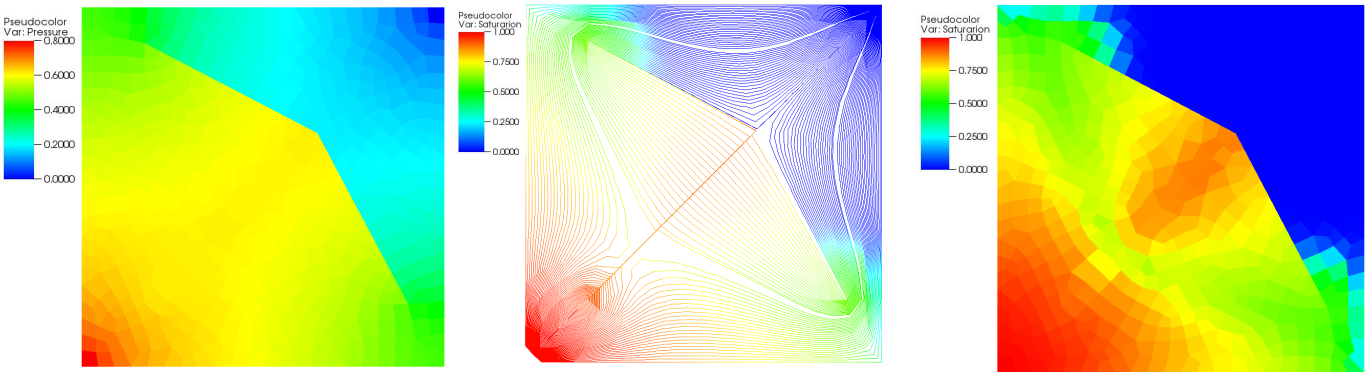

Figure 8. Pressure and Saturation fields using the MPFA-D/SF-HyG for the for the ¼ of five-spot problem with connected channel and barriers at t = 0.5 PVI: (a) Pressure field. (b) Streamlines Saturation. (c) Saturation field.

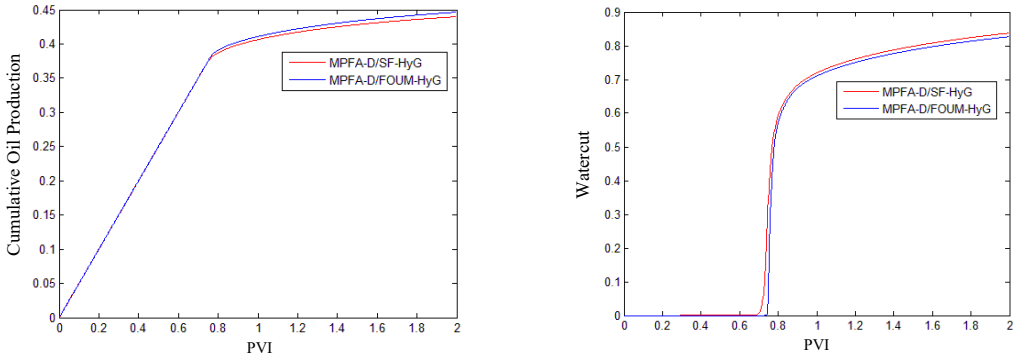

(a) (b)

Figure 9. Production report for the ¼ five spot two-phase flow problem with connected channel and barriers. (a) Cumulative Oil Production. (b) Watercut

5. CONCLUSIONS

In this work, we have presented a formulation for the numerical simulation of two-phase fluid flows in naturally fractured petroleum reservoirs. To represent the fracture network, we have used a Hybrid Grid model (HyG). To solve the elliptic pressure equation in the fractured media, we used a Finite Volume based in a Multipoint Flux

Approximation with a Diamond Stencil (MPFA-D). The hyperbolic saturation equation was spatially discretized by Streamline formulation (SF). In order to evaluate the effectiveness of our MPFA-D/SF-HyG formulation we have solved some two-phase flow problems using unstructured quadrilateral meshes. For the examples tested and other not shown in the present paper, our results are very similar to other formulations found in literature showing the potential of our method to obtain very accurate results at a reasonable computational cost.

6. REFERENCES

Ahmed, R., Edwards, M. G., Lamine, S., Huisman, B. A. H. and Pal, M. (2017). CVD-MPFA full pressure support, coupled unstructured discrete fracture-matrix Darcy-flux approximations. *J. Comput. Phys.*

Aziz, K and Settare, A. (1979). Petroleum Reservoir Simulation, New York.

Batycky, R. P. (1997). Three-Dimensional Two-Phase Field Scale Streamline Simulator. *PhD Thesis,* 163 p.

Bear, J. (1972). Dynamics of Fluids in Porous Media, New York: Dover Publications Inc.

Blunt, M.J., Lui, K., Thiele, M.R. (1996). A Generalized Streamline Method to Predict Reservoir Flow. *Petroleum Geoscience*, 259–269.

Cavalcante, T. M., Contreras, F. R. L., Lyra, P. R. M., and Carvalho D. K. E. de.; (2018) A MPFA-D Finite Volume Scheme for the 2-D Simulation of Fluid Flows in Naturally Fractured Reservoirs Using a Hybrid-Grid Fracture Model. *International Journal for Numerical Methods in Fluids* (To appear).

Chen, H., Onishi, T., Olalotiti-Lawal, F. and Datta-Gupta, A. (2018) Streamline Tracing and Applications in Naturally Fractured Reservoirs Using Embedded Discrete Fracture Models. *SPE Annual Technical Conference and Exhibition*. Dallas, Texas, 24-26.

Chen, Z., Huan, G., Ma, Y. (2006). *Computational Methods for Multiphase Flows in Porous Media.* Dallas: SIAM

Contreras, F. R. (2012). A cell-centered finite volume method for the simulation of two-phase flows in heterogeneous and anisotropic oil reservoirs. *Master Thesis (In Portuguese)*. Recife: UFPE.

Contreras, F. R. L., Lyra, P. R. M., Souza, M. R. A and Carvalho, D. K. E. (2016). A cell-centered multipoint flux approximation method with a diamond stencil coupled with a higher order finite volume method for the simulation of oil–water displacements in heterogeneous and anisotropic petroleum reservoirs. *Computers & Fluids,* vol. 127, p. 1–16.

Cordes, C. and Kinzelbach, W. (1992). Continuous groundwater velocity fields and path lines in linear, bilinear and trilinear finite elements. *Water Resourcers Reserarch*, v. 28, n. 11, p. 2903–2911.

Da Silva, R. S., Lyra, P. R. M., Willmersdorf, R. B., and de Carvalho, D. K. E. (2016). A higher resolution edge-based finite volume method for the simulation of the oil-water displacement in heterogeneous and anisotropic porous media using a modified IMPES method. *International Journal for Numerical Methods in Fluids*, 82(12), 953–978.

Datta-Gupta, A. and King, J. (2007). Streamline simulation: theory and practice. n 11. SPE Textbook Series.

Ewing, R. E. (1983). The Mathematics of Reservoir Simulation, Philadelphia: SIAM.

Firoozabadi, A. (2000). Recovery Mechanisms in Fractured Reservoirs and Field Performance. *Journal of Canadian Petroleum Technology*, 39(11).

Gao, Z., and Wu, J. (2010). A linearity-preserving cell-centered scheme for the heterogeneous and anisotropic diffusion equations on general meshes. *Int. J. Numer. Methods Fluids, 67*, 2157–2183.

Hægland, H., Dahle, H.K., Eigestad, G.T., Lie, K.A., Aavatsmark, I. (2007) Improved streamlines and time-of-flight for streamline simulation on irregular grids. *Advances in Water Resources.* 1027–1045.

Hirsch, C. (1994) Numerical Computation of Internal and External Flows, Brussels: Wiley.

Hurtado, F.S.V., Maliska, C.R., Silva, A.F.C. (2006). A Variable Timestep Strategy for Accelerating the IMPES Solution Algorithm in Reservoir Simulation*. XXVI Iberian Latin-American Congress on Computational Methods in Engineering (CILAMCE).*

Jimenez, E., Sabir, K., Datta-Gupta, A., and King, M. J. (2007). Spatial Error and Convergence in Streamline Simulation. *SPE Reservoir Simulation Symposium. Society of Petroleum Engineers.* 12 p.

Kozdon, J. E., Mallison, B. T. and Gerritsen, M. G. (2011). Multidimensional upstream weighting for multiphase transport in porous media. *Comput. Geosci.,* vol. 15, p. 399–419.

Mesbah, M., Vatani, A., Siavashi, M. (2018) Streamline simulation of water-oil displacement in a heterogeneous fractured reservoir using different transfer functions. *Oil and Gas Science and Technology*.

Peaceman, D. W. (1977). Fundamentals of Numerical Reservoir Simulation. *Elsevier Scientific Publishing.*

Pollock, D.W. (1988). Semianalytical computation of path lines for finite difference models. *Ground Water Jornal.*

Sandve, T. H., Berre, I. and Nordbotten, J. M. (2012). An efficient multi-point flux approximation method for discrete fracture-matrix simulations. *J. Comput. Phys.,* vol. 231, no. 9, p. 3784–3800.

Thiele, M. R., Batycky, R. P., Blunt, M.J., and Orr, F. M.: (1996). Simulating Flow in Heterogeneous Media Using Streamtubes and Streamlines. *SPE Reservoir Engineering*. no. 1, p. 5–12.

7. RESPONSIBILITY NOTICE

The authors are the only responsible for the printed material included in this paper.